PCCP

Accepted Manuscript

ROYAL SOCIETY OF CHEMISTRY

www.rsc.org/pccp

Journal Name

RSCPublishing

ARTICLE

Modulation of Physical Properties in Supramolecular Hydrogels Based on Hydrophobic Core

Cite this: DOI: 10.1039/x0xx00000x

Keigo Matsumoto,[a,b*] Atsuomi Shundo,[c,d] Masashi Ohno,[b] Shun Fujita,[b] Kowichiro Saruhashi,[b] Nobuhide Miyachi,[b] Katsuaki Miyaji[b] and Keiji Tanaka[a,c,d,*]

Received 00th January 2012,
Accepted 00th January 2012

DOI: 10.1039/x0xx00000x

www.rsc.org/

We demonstrate herein variation in viscoelastic properties of supramolecular hydrogels (SMGs) composed of two amphiphiles, *N*-Palmitoyl-Gly-His (PalGH) and sodium palmitate (PalNa). PalGH molecules in water form lamellar-like assemblies, which stack into sheet-shaped aggregates, resulting in the evolution of three-dimensional network structures. Once PalNa is added into PalGH, alkyl groups of PalNa incorporate themselves into hydrophobic cores of PalGH lamellar-like assemblies, which causes a change in the assembly from lamellar-like to fibrous micelle-like. Consequently, sheet-shaped aggregates turn into flexible fibrils, which form bundles, resulting in network structures. Mixed hydrogel network structures differ in morphology from those in homogenous PalGH and PalNa hydrogels. Changes in network structure eventually alter the bulk viscoelastic properties of hydrogels. These results demonstrate that the viscoelastic properties of supramolecular hydrogels can be tuned by controlling aggregation states.

1. Introduction

Supramolecular hydrogels (SMGs), in which amphipihilic molecules form a three-dimensional network, have been studied as a class of soft materials capable of immobilizing a large amount of water within a network. In SMGs, molecules self-assemble by non-covalent interactions such as hydrogen bonds, hydrophobic effects, van der Waals interactions, π-π interactions, and/or electrostatic interactions. Thus, the physical properties of SMGs can remarkably vary in relation to external stimuli including temperature,[1] pH,[2] solvent polarity[2b,3] and mechanical stress or strain.[4] Due to this tunable feature, SMGs are promising candidates for many applications such as injectable gels for tissue engineering,[5] carriers for drug delivery,[6] self-healing materials,[7] separation medium[8] and so forth.

One of the common strategies to obtain SMGs with tailored physical properties is the chemical modification of molecules, which form gels, and so-called gelators. So far, a great effort has been made to study correlations between chemical structures of molecules and physical properties of hydrogels.[9] Such an approach has provided a better understanding of how to control physical properties of hydrogels by modifying chemical structures. For the moment, however, it is still difficult to obtain hydrogels with desired properties based on the design of gelator molecules.

Recently, SMGs composed of two kinds of molecules, named two-component gels, have attracted much attention.[10] In two-component gels, two molecules co-assemble into fibrous network structures. This means that the co-assembly offers an additional level of control in the hierarchical assembly process and has the potential for exquisite tunability, which cannot be achieved by one-component gels.[11] In addition, aggregation states and physical properties of assemblies can be easily tuned by varying composition ratios of the two molecules.

In this study, we report on a SMG composed of *N*-Palmitoyl-Gly-His (PalGH) and sodium palmitate (PalNa). PalGH molecules in water form lamellar-like assemblies, which stack into sheet-shaped aggregates, resulting in the evolution of three-dimensional network structures. PalNa was chosen as a modulator for the lamellar-like assembly of PalGH, because alkyl groups of PalNa should incorporate into hydrophobic cores in assemblies of PalGH, leading to changes in the hierarchical structure, thereby the bulk physical properties of hydrogels. The usage of a hydrophobic moiety as a modulator for the gelator assembly is unlike most of the work that has been published so far, in which a hydrophilic moiety has been used,[12] and is featured in this current work.

2. Experimental

2.1 Materials

Sodium palmitate (PalNa) purchased from Chem Service Inc. was used as received. *N*-Palmitoyl-Gly-His (PalGH) was synthesized according to a previously-reported method.[13] Water was deionized with Elix UV3 (Millipore Co.), and used for hydrogel formation. Deuterated water (D_2O) and dimethyl sulfoxide (DMSO-d_6) were purchased from SIGMA-Aldrich Co. LLC., and were used for Fourier-transform infrared (FT-IR) spectroscopy. For confocal laser scanning microscopy (CLSM), 9-(diethylamino)-5H-benzo[a]phenoxazin-5-one (Nile Red) was purchased from Tokyo Chemical Industry Co. Ltd., and was used as received.

2.2 Gel preparation

PalGH and/or PalNa were well-dispersed into 4 mL of pure water and heated at 373 K for 1 h in a dry bath incubator (AS ONE Co. Ltd.). To suppress the water evaporation, sealed vials were used (AS ONE Co. Ltd.). The weight loss caused by the water evaporation was less than 0.3 %. The resulting clear solution was left undisturbed for 19 hours at room temperature, to obtain hydrogels. Keeping the PalGH concentration to be 20 mM, the molar percentage of PalNa in hydrogels (*X*) was varied; 0, 20, 50 and 100 %.

2.3 Rheological measurements

Rheological measurements were made using an Anton Parr MCR 301 rheometer (Anton Paar Japan K.K). In all measurements, a cone-typed plate with a diameter of 50 mm and a tilt angle of 1.0° was used. A piece of paper wet with water was laid around the sample to prevent water evaporation from samples during measurements. An aqueous solution of PalGH and/or PalNa pre-warmed at 373 K was mounted on a sample stage, which was controlled at a temperature of 333 K. The solution was sandwiched between a cone-typed plate and a flat stage, and aged at 298 K. After the completion of gelation (20 min for a PalNa system and 5 hours for the others), frequency and strain sweeps were performed.

2.4 Fourier-transform infrared spectroscopy

For the FT-IR measurements, PalGH and/or PalNa were/was dissolved in D_2O by heating at 373 K. The resultant hot solution was sandwiched between CaF_2 windows with a 0.1 mm-gap and was aged at room temperature for 90 min. Also, the DMSO-d_6 solution of PalGH sandwiched between CaF_2 windows was prepared as a reference sample. The FT-IR spectra were recorded with a FT/IR-620 spectrometer (JASCO Co.) equipped with a triglycine sulfate (TGS) detector. All spectra were obtained with a resolution of 4 cm^{-1} and 64 scans at room temperature.

2.5 Small-angle X-ray scatting measurements

Small-angle X-ray scatting (SAXS) experiments were carried out at the BL40B2 beamline of SPring8 (Japan). The wavelength of incident X-rays and the sample-to-detector distance were 0.15 nm and 1669 mm, respectively. Hydrogels prepared in a quartz capillary were placed in a sample stage. Scattered X-rays were recorded using a Rigaku R-AXIS IV+++ system (300 × 300 mm imaging plate). Exposure times for homo PalNa hydrogel and others were 600 and 300s, respectively. By circular averaging the two-dimensional pattern on the imaging plate, a one-dimensional scattering profile of the sample was obtained.

2.6 Transmission electron microscopy

A hydrogel sample was placed on a carbon-coated copper grid (Alliance Biosystems Co. Ltd.) and was dried under an ambient atmosphere. The specimen was further coated with carbon by a CADE-E coater (Meiwafosis Co. Ltd.). Transmission electron microscopic (TEM) images were recorded with a H8000 Scanning Transmission Electron Microscope (Hitachi High-technologies Co. Ltd.). Observations were carried out with an acceleration voltage of 200 kV.

2.7 Confocal laser scanning microscopy

An aqueous solution of each sample containing 60 μM of Nile Red pre-warmed at 373 K was placed in a glass bottom dish (Matsunami Glass Inc. Ltd.) and sealed with a glass cover using vacuum grease. The sample was left undisturbed for 5 hours to equilibrate to room temperature prior to observation with a confocal laser scanning microscope (CLSM) equipped with a semiconductor laser and a DAPI filter block (LSM700, Carl Zeiss Microscopy Co., Ltd.).

3. Results and discussion

3.1 Gel preparation

Fig. 1 shows the chemical structure of PalGH and PalNa together with photographs showing hydrogels composed of PalGH and PalNa. To address the effect of PalNa on gel formation, the PalNa concentration was varied at 0 mM, 5 mM and 20 mM while the PalGH concentration was kept at 20 mM. Thus, the molar percentages of PalNa in hydrogels (*X*) were 0, 20, 50 and 100 %.[14]

When PalGH was dissolved in water by heating at 373 K and then subsequently cooled slowly to room temperature, it formed hydogels. This was also the case for PalNa. In both

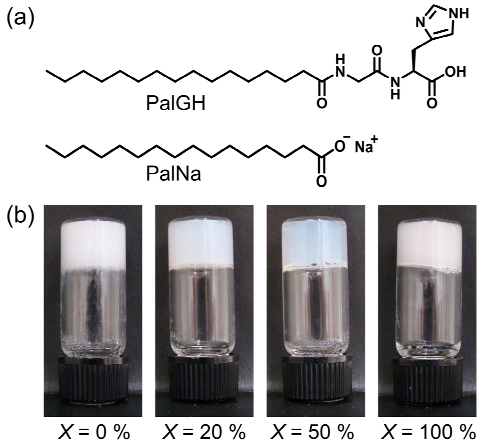

Fig. 1 (a) Chemical structures of hydrogelators, *N*-palmitoyl-Gly-His (PalGH) and sodium palmitate (PalNa). (b) Photographic images of hydrogels with various compositions of PalNa (*X* = 0, 20, 50 and 100 %).

cases, the appearance of hydrogels was nebulous, suggesting that the scattering of visible light occurred due to the presence of molecular aggregations with relatively-large size. With increasing PalNa concentration in hydrogels, however, the hydrogel became more transparent. This indicates that the size of the molecular aggregations decreased upon addition of the PalNa.

3.2 Viscoelastic properties

The change in the apparent transparency of hydrogels motivated us to examine the viscoelastic properties of hydrogels with different molar percentages of PalNa (X = 0, 20, 50 and 100 %). Fig. 2 shows the storage and loss moduli (G' and G'') as a function of frequency (ω), obtained using a strain amplitude (γ) of 0.05 %. For all hydrogels, G' was larger than G'' at a given frequency and they did not cross-over, even in the low frequency regions employed. This behavior is a signature that the systems exist in rigid gel states.[15]

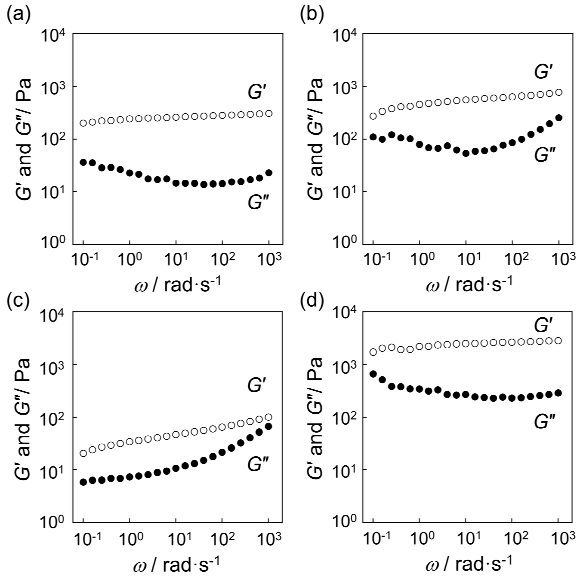

Fig. 2 Frequency dependence of storage and loss moduli (G' and G'') obtained for hydrogels with (a) X = 0, (b) 20, (c) 50 and (d) 100 % at a strain amplitude of 5x10^{-2} %. Filled and open circles denote G' and G'', respectively.

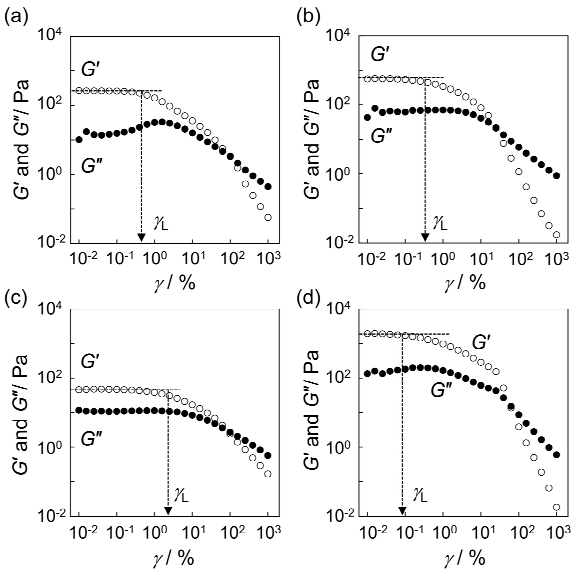

Fig. 3 Strain dependence of storage and loss moduli (G' and G'') obtained for hydrogels with (a) X = 0, (b) 20, (c) 50 and (d) 100 % at an angular frequency of 1.0 rad·s^{-1}. Filled and open circles denote G' and G'', respectively.

Fig. 3 shows G' and G'' plotted against γ using ω = 1.0 rad·s^{-1}. For the homogenous PalGH hydrogel (X = 0 %), the G' value was almost constant around 260 Pa at a low γ below 0.4 %. In this region, G' was larger than G'', indicating that the hydrogel behaved as an elastic solid. However, when γ went beyond 0.4 %, G' started to decrease with increasing γ, resulting in $G' < G''$ at a high γ. This suggests that the molecular assemblies and/or their aggregated structures were, in part, broken by large deformations. Such was also the case for homogenous PalNa hydrogels (X = 100 %).

Strain dependences of G' and G'' were also observed for mixed hydrogels with X = 20 and 50 %. However, the G' value at a plateau region, or at a low γ, (G'_p) and limiting strain amplitude (γ_L), where G' was no longer constant with increasing γ, were dependent on the value of X. The G'_p value observed at X = 20 % (G'_p = 570 Pa) was larger than that observed at X = 0 % (G'_p = 260 Pa) although the γ_L value were almost comparable to each other. When the PalNa concentration further increased to X = 50 %, the G'_p value turned to decrease to 50 Pa. In this case, however, the γ_L value of 1.1 % was larger than 0.4 % for X = 0 %, indicating that the hydrogel is more persistent in the strain before the deformation. Thus, it can be claimed that viscoelastic properties of PalGH hydrogels could be regulated by the PalNa concentration.

3.3 Molecular assembled states

Molecular aggregation states of hydrogels with various compositions were examined. Fig. 4 shows the FT-IR spectra for hydrogels with X = 0, 20, 50 and 100 %. For comparison, spectra for PalGH dissolved in dimethyl sulfoxide (DMSO) are also shown. Deuterated solvents were used for the preparation of all samples and then the contribution from the solvent was removed by subtracting the solvent spectrum corrected using a

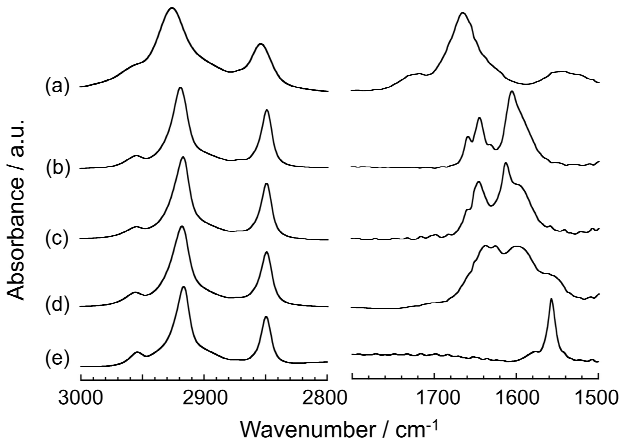

Fig. 4 FT-IR spectra of (a) PalGH in DMSO and hydrogels composed of PalGH and PalNa with (b) X = 0, (c) 20, (d) 50 and (e) 100 %. Each spectrum is normalized and is horizontally shifted for the sake of clarity.

scaling factor.

For the homo PalGH hydrogel (X = 0 %), absorption peaks assignable to the symmetric and antisymmetric C-H stretching vibrations of methylene groups (ν_s,CH_2 and ν_{as},CH_2) appeared at 2849 and 2919 cm^{-1}, respectively. These values were smaller than those obtained for the DMSO solution (2854 and 2925 cm^{-1}) where the PalGH molecules homogeneously dispersed. This indicates that the alkyl chain in PalGH was extended with a higher population in the *trans* conformation in the hydrogel. Also, the homo PalGH hydrogel exhibited peaks due to the C=O stretching vibration in the amide moiety ($\nu_{C=O}$) at two different wavenumbers, 1645 and 1605 cm^{-1}. Another peak at 1658 cm^{-1}, which arose from the vibration of the C=O group in the carboxyl group (ν_{COOH}), was also observed. On the other hand, the DMSO solution provided the $\nu_{C=O}$ peak at 1665 cm^{-1}, which also included in part the ν_{COOH} peak. The position of two $\nu_{C=O}$ peaks observed for the hydrogel is lower than that for the DMSO solution. This is a solid signature that the C=O groups form hydrogen bonds with each other.[16] Thus, it is most likely that the two $\nu_{C=O}$ peaks observed for the PalGH hydrogel are assignable to C=O groups, which form weak and strong hydrogen bonds, respectively.

The peak positions of ν_s,CH_2 and ν_{as},CH_2 were independent of the X value. Taking into account that the peak positions observed for hydrogels with X = 0 and 100 % were identical to each other, the X-independence in the peak position can be understood. However, such was not the case for peaks located in the range of 1800-1500 cm^{-1}. With increasing X to 50 %, peaks at 1645 and 1605 cm^{-1}, which were due to $\nu_{C=O}$ of PalGH, respectively, shifted to lower and higher wavenumbers (1645 and 1613 cm^{-1} for X = 20 %; 1637 and 1626 cm^{-1} for X = 50 %). This indicates that hydrogen bonds among the amide moieties in PalGH become stronger and weaker, respectively, upon the addition of PalNa. Also, the addition of PalNa into the PalGH hydrogel caused the intensification of broad peaks centered at 1600 cm^{-1} and 1564 cm^{-1} with a concurrent decrease in the intensity of the ν_{COOH} peak at 1658 cm^{-1}. The peaks at 1600 cm^{-1} and 1564 cm^{-1} are assignable to the vibration of the C=O group the carboxylates (ν_{COO^-}) in PalGH and PalNa, respectively. The intensification of the ν_{COO^-} peak accompanied by the intensity decrease of the ν_{COOH} peak suggests that the carboxyl group in PalGH was deprotonated upon addition of PalNa. Here, an important fact is that the spectrum for hydrogels composed of PalGH and PalNa cannot be simply expressed by overlapping two spectra for the homo PalGH and PalNa hydrogels. This implies that the PalNa molecules incorporate into the PalGH assembly, accompanied by changes in the strength of the hydrogen bonding and the protonation state of the carboxylate.[17]

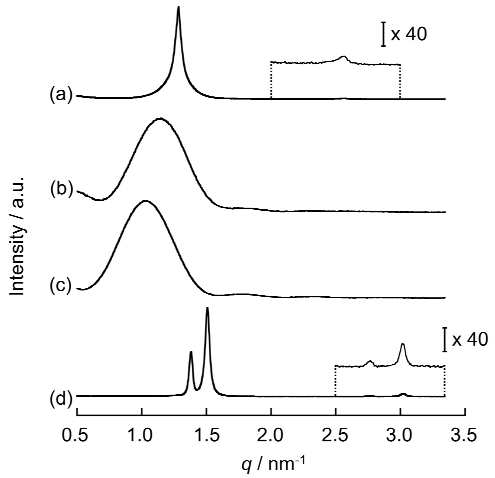

Fig. 5 SAXS profiles of hydrogels with (a) X = 0, (b) 20, (c) 50 and (d) 100 %. Each curve is normalized and is horizontally shifted for clarity.

Fig. 5 shows SAXS profiles for hydrogels with X = 0, 20, 50 and 100 %. In the case of the homo PalGH hydrogel (X = 0 %), sharp peaks were observed at a scattering vector (q) of 1.3 and 2.6 nm^{-1}, respectively, corresponding to the domain spacing (d) of 4.9 and 2.4 nm. These peaks obey the characteristic position ratio of 1:2. Invoking that the peaks at q of the ratio 1:2:3:4 etc. are characteristic of a lamellar system,[18] it is conceivable that PalGH molecules form a lamellar assembly with an interlayer distance of 4.9 nm. The lamellar assemblies were also found in the homogenous PalNa hydrogel (X = 100 %), which provided two sets of peaks located at q = 1.4 and 1.5 nm^{-1} as the first-order peak (d = 4.5 and 4.2 nm). Such lamellar assemblies with two different interlayer distances might have arisen from the two different forms, protonation and deprotonation, of the carboxyl groups in the PalNa molecules, as observed for the other saturated fatty acids.[19]

In the case of hydrogels with X = 20 and 50 %, sharp peaks due to the lamellar assembly were replaced by a broad peak. The peak was observed at q = 1.1 nm^{-1} (d = 5.5 nm) for X = 20 % and q = 1.0 nm^{-1} (d = 6.1 nm) for X = 50 %. The broad scattering pattern cannot be simply explained in terms of an increase in the interlayer distance of the lamellar assembly. In general, the broadening of a peak reflects that moieties have relatively high electron density are not uniformly distributed in the periodic structure.[20] Such a distribution was often the case for micelle-like assemblies with a large aspect ratio, formed by amphiphilic molecules.[4c,4d,21] Thus, it seems reasonable to predict that the incorporation of the palmitoyl groups of PalNa into the lamellar-like assembly of PalGH leads to the formation of a fibrous micelle-like co-assembly.

3.4 Morphology of aggregates and network structure

To confirm the change in the PalGH assembly upon addition of PalNa, transmission electron microscopic (TEM) observations were made. Fig. 6 shows TEM images obtained for hydrogels with X = 0, 20, 50 and 100 %. In the case of the homo PalGH hydrogel (X = 0 %), sheet-shaped aggregates were observed. The width, length and thickness of the aggregates were 77 - 190 nm, > 910 nm and 31 - 38 nm, respectively. Sheet-shaped aggregates were also observed for the homo PalNa hydrogel with (X = 100 %) although the morphology differs from that for the homo PalGH. In this case, the width, length and thickness of the aggregates were 54 - 190 nm, > 7.1 μm, and 45 nm, respectively. Given that the lamellar assemblies stacked each other, the formation of sheet-shaped aggregates can be reasonably understood.[22]

The addition of PalNa to PalGH hydrogels induced changes in morphology from sheets to fibrils. At X = 20 %, the

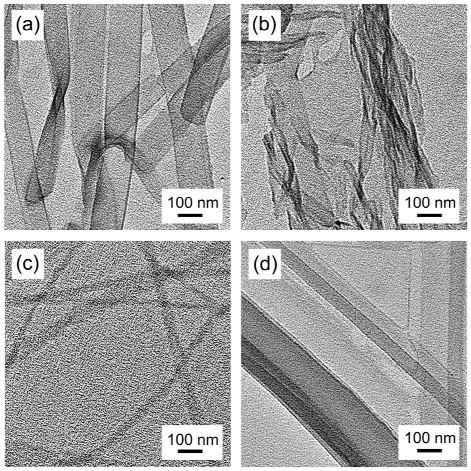

Fig. 6 (a) TEM images of aggregates in hydrogels with (a) $X = 0$, (b) 20, (c) 50 and (d) 100 %.

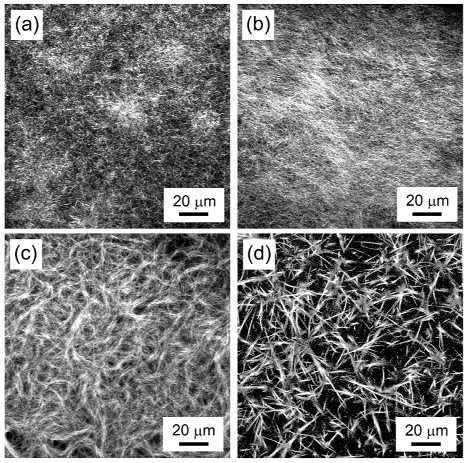

Fig. 7 Confocal laser scanning microscopic images of hydrogels with (a) $X = 0$, (b) 20, (c) 50 and (d) 100 %, which contain Nile Red as a fluorescence probe dye. The concentration of Nile Red was 60 μM.

hydrogel showed an intermediate state between the two morphologies, as evidenced by the presence of both sheets and fibrils. When the concentration of PalNa increased up to X = 50 %, all of the sheets turned to fibrils with widths of 15 - 160 nm, lengths > 5.5 μm and thicknesses of 23 - 31 nm. These observations support that the PalGH and PalNa co-assembled into fibrils. Or otherwise, two kinds of sheets with different shapes would be observed. TEM observations are in good accordance with the results obtained using FT-IR spectroscopy and SAXS measurements.

We finally come to the network structure of aggregates by confocal laser scanning microscopy (CLSM). As a fluorescence probe, 9-(diethylamino)-5H-benzo[a]phenoxazin-5-one (Nile Red) was used. This dye is hardly soluble in pure water and localizes in hydrophobic cores of molecular assemblies.[23] This feature makes it possible to stain the assembly and to give a contrast in a fluorescence microscopic image.[24] Fig. 7 shows CLSM images obtained for hydrogels with X = 0, 20, 50 and 100 %. Both in the homo PalGH and PalNa hydrogels (X = 0 and 100 %), fibrils and their networks were observed although the fibril size was not the same in the two gels; the size of fibrils formed by PalGH were smaller than those of PalNa.[25] Taking into account the resolution of CLSM, the morphology of fibrils should not be discussed here. However, based on TEM observations, it is plausible that fibrils observed in both hydrogels should be sheet-like in shape.

In mixed hydrogels with X = 20 %, fibrils and their networks were also observed. Although the fibril size was comparable to that for the homo PalGH hydrogel, fibrils existed more densely, as evidenced by dense white regions in CLSM images. With increasing PalNa concentration to X = 50 %, fibrils aggregated into a bundle with more flexibility and bundles led to the formation of network structures. Thus, it can be claimed that the molecular-level modulation of the PalGH assembly by using PalNa was amplified to induce microscopic network structures in hydrogels.[26]

3.5 Relationship between network structure and viscoelastic properties

Finally, we discuss the relationship between fibril network structures and viscoelastic properties for resulting hydrogels. According to MacKintosh *et al.*, G'_p of physical gels can be expressed by the following equation:[27]

$$G'_p \sim \frac{\kappa^2}{k_B T} \xi^{-2} L_e^{-3} \quad (1)$$

where κ is bending modulus of the fibrils, ξ is mesh size in the network, L_e is entanglement length, k_B is Boltzmann constant and T is absolute temperature. The CLSM observation revealed that, for the mixed hydrogel with X = 20 %, fibrils exist more densely than those for the homogenous PalGH hydrogel (X = 0 %). Such an increase in the fibril density should decrease the values of ξ and L_e. Based on the equation (1), a higher G'_p value can be predicted from smaller ξ and L_e. This is exactly what we obtained using the rheological measurements, as shown in Fig. 3. That is, the G'_p value of the mixed hydrogel with X = 20 % (G'_p = 570 Pa) was larger than that of X = 0 % (G'_p = 260 Pa).

With increasing PalNa concentrations, at X = 50 %, fibrils become more flexible and form bundles, as shown in Fig. 7. Higher flexibility of the fibrils and their bundles corresponds to smaller κ values. Then, smaller κ values result in smaller G'_p. This is in good accordance with the experimental result that the mixed hydrogel with X = 50 % provided smaller G'_p values (G'_p = 50 Pa) compared with other hydrogels.

The different γ_L values depending on the PalNa concentration in mixed hydrogels should be discussed. As mentioned above, the γ_L value for the mixed hydrogel with X = 50 % was 1.1 % thus larger than 0.4 % for the homo PalGH hydrogel and 0.2 % for the X = 20 % mixed hydrogel. The strain response of supramolecular hydrogels is related to the cross-liking points in the network structure. For example, effective entanglements and/or interactions of molecular-assembled fibrils, which behave as cross-liking points, were more persistent to the deformation, leading to a higher γ_L value.[28] In the mixed hydrogel with X = 50 %, fibrils stacked each other to produce bundles. When considering that the

bundle formation represents evidence for the strong interaction between fibrils, the higher γ_L value at X =50 % can be reasonably understood.

4. Conclusions

We demonstrated variations in viscoelastic properties of supramolecular hydrogels composed of *N*-Palmitoyl-Gly-His (PalGH) and sodium palmitate (PalNa). The stiffness and the strain response of mixed hydrogels could be regulated by the PalNa concentration. The increase of the PalNa concentration changed the molecular assembly from lamellar-like to fibrous micelle-like. Consequently, sheet-shaped aggregates turned to fibrils. Fibrils formed a flexible bundle and bundles led to network formation, which differed from those for the homo PalGH and PalNa hydrogels. Such a network structure can be associated with the bulk viscoelastic properties of mixed hydrogels. These results illustrate that the molecular-level modulation of the assembly was amplified to induce the microscopic network structure, thereby the viscoelastic properties of the hydrogel. It should be noted that the modulation of the molecular assembly was based on the incorporation of alkyl groups from PalNa molecules into hydrophobic cores of PalGH assemblies. In most two-component gels reported so far, interactions between the hydrophilic moieties of two molecules were generally utilized as a driving force to control the molecular assembly. Thus, findings in this study are novel and should provide useful concepts in the development of supramolecular hydrogels with desired physical properties by the modulation of hydrophobic cores of molecular assemblies.

Acknowledgements

The synchrotron radiation facilities experiments were performed at BL40B2 in the SPring8 with the approval of the Japan Synchrotron Radiation Research Institute (JASRI) (Proposal: 2012A1522). We thank Prof. Masahiro Goto and Dr. Rie Wakabayashi at Kyushu University for supporting this work with the use of confocal laser scanning microscopy. This research was partly supported by a Grant-in-Aid for Scientific Research (B) (No. 24350061) from the Ministry of Education, Culture, Sports, Science and Technology, Japan.

References

[a] *Department of Automotive Science, Kyushu University, Fukuoka 819-0395, Japan*
[b] *Nissan Chemical Industries, Ltd., Tokyo 101-0054, Japan; E-mail: matsumotoke@nissanchem.co.jp*
[c] *Department of Applied Chemistry, Kyushu University, Fukuoka 819-0395, Japan; E-mail: k-tanaka@cstf.kyushu-u.ac.jp*
[d] *International Institute for Carbon-Neutral Energy Research (WPI-I2CNER), Kyushu University, Fukuoka 819-0395, Japan*

1. (*a*) S. Kiyokawa, K. Sugiyasu, S. Shinkai and I. Hamachi, *J. Am. Chem. Soc*., 2002, **124**, 10954; (*b*) G. Graf, S. Drescher, A. Meister, B. Dobner and A. Blume, *J. Phys. Chem. B*, 2011, **115**, 10478.
2. (*a*) S. R. Haines and R. G. Harrison, *Chem. Commun*., 2002, **23**, 2846; (*b*) H. Komatsu, S. Matsumoto, S. Tamaru, K. Kaneko, M. Ikeda and I. Hamachi, *J. Am. Chem. Soc*., 2009, **131**, 5580; (*c*) T. Ratra, A. Pal and J. Dey, *Langmuir*, 2010, **26**, 7761; (*d*) J. Raeburn, G. Pont, L. Chen, Y. Cesbron, R. Lévy and D. J. Adams, *Soft Matter*, 2012, **8**, 1168; (*e*) D. M. Wood, B. W. Greenland, A. L. Acton, F. R. Llansola, C. A. Murray, C. J. Cardin, J. F. Miravet, B. Escuder, I. W. Hamley and W. Hayes, *Chem. Eur. J*., 2012, **18**, 2692.
3. (*a*) A. R. Hirst and D. K. Smith, *Langmuir*, 2004, **20**, 10851; (*b*) D. K. Kumar, D. A. Jose, A. Das and P. Dastidar, *Chem. Commun*., 2005, **32**, 4059; (*c*) N. A. Dudukovic and C. F. Zukoski, *Langmuir*, 2014, **30**, 4493.
4. (*a*) A. P. Nowak, V. Breedveld, L. Pakstis, B. Ozbas, D. J. Pine, D. Pochan and T. J. Deming, *Nature*, 2002, **417**, 424; (*b*) M. Yoshida, N. Koumura, Y. Misawa, N. Tamaoki, H. Matsumoto, H. Kawanami, S. Kazaoui and N. Minami, *J. Am. Chem. Soc*., 2007, **129**, 11039; (*c*) D. P. Penaloza, A. Shundo, K. Matsumoto, M. Ohno, K. Miyaji, M. Goto and K. Tanaka, *Soft Matter*, 2013, **9**, 5166; (*d*) A. Shundo, Y. Hoshino, T. Higuchi, Y. Matsumoto, D. P. Penaloza Jr, K. Matsumoto, M. Ohno, K. Miyaji, M. Goto and K. Tanaka, *RSC Adv*., 2014, **4**, 36097.
5. S. Ziane, S. Schlaubitz, S. Miraux, A. Patwa, C. Lalande, I. Bilem, S. Lepreux, B. Rousseau, J. L. Meins, L. Latxague, P. Barthelemy and O. Chassande, *Eur. Cell Matter*., 2012, **23**, 147.
6. (*a*) X. Xu, L. Liang, C. S. Chen, B. Lu, N. Wang, F. G. Jiang, X. Z. Zhang and R. X. Zhuo, *ACS Appl. Matter. Interfaces*, 2010, **2**, 2663; (*b*) S. Soukasene, D. Toft, T. J. Moyer, H. Lu, H. K. Lee, S. M. Standley, V. L. Crynes and S. Stupp, *ACS Nano*, 2011, **5**, 9113; (*c*) A. Baral, S. Roy, A. Dehsorkhi, I. W. Hamley, S. Mohapatra, S. Ghosh and A. Banerjee, *Langmuir*, 2014, **30**, 929; (*d*) J. Liu, J. Liu, L. Chu, Y. Zhang, H. Xu, D. Kong, Z. Yang, C. Yang and D. Ding, *ACS Appl. Matter. Interfaces*, 2014, **6**, 5558.
7. (*a*) A. Pasc, P. Gizzi, N. Dupuy, S. Parant, J. Ghanbaja and C. Gérardin, *Tetrahedron Lett*., 2009, **50**, 6183; (*b*) A. Shundo, K. Mizuguchi, M. Miyamoto, M. Goto and K. Tanaka, *Chem. Commun*., 2011, **47**, 8844; (*c*) S. Roy, A. Baral, A. Banerjee, *Chem. Eur. J*., 2013, **19**, 14950.
8. C. Yang, D. Li, Z. Liu, G. Hong, J. Zhang, D. Kong and Z. Yang, *J. Phys. Chem. B*, 2011, **116**, 633.
9. (*a*) L. Chen, S. Revel, K. Morris, L. C. Serpell and D. J. Adams, *Langmuir*, 2010, **26**, 13466; (*b*) D. M. Ryan, S. B. Anderson and B. L. Nilsson, *Soft Matter*, 2010, **6**, 3220; (*c*) H. Wang, C. Yang, M. Tan, L. Wang, D. Kong and Z. Yang, *Soft Matter*, 2011, **7**, 3897.
10. (*a*) X. Y. Liu and P. D. Sawant, *Angew. Chem. Int. Ed.*, 2002, **41**, 3641; (*b*) G. O. Lloyd and J. W. Steed, *Nature Chem*., 2009, **1**, 437; (*c*) L. Chen, S. Revel, K. Morris, D. G. Spiller, L. C. Serpell and D. J. Adams, *Chem. Commun*., 2010, **46**, 6738; (*d*) D. M. Ryan, T. M. Doram and B. L. Nilsson, *Langmuir*, 2011, **27**, 11145; (*e*) B. Adhikari, J. Nande and A. Banerjee, *Soft Matter*, 2011, **7**, 8913; (*f*) L. E. Buerkle and S. J. Rowan, *Chem. Soc. Rev.*, 2012, **41**, 6089; (*g*) G. Pont, L. Chen, D. G. Spiller and D. J. Adams, *Soft Matter*, 2012, **8**, 7797; (*h*) J. A. Foster, R. M. Edkins, G. J. Cameron, N. Colgin, K. Fucke, S. Ridgeway, A. G. Crawfod, T. B. Marder, A. Beeby, S. L. Cbb and J. W. Steed, *Chem. Eur. J*., 2014, **20**, 279; (*i*) D. Li, Y. Shi and L. Wang, *Chin. J. Chem*., 2014, **32**, 123.
11. (*a*) M. D. Barry, R. C. Rowe, *Int. J. Pharm*., 1989, **53**, 139; (*b*) J. Merta, B. A. Coldren, H. Warriner, R. van Zanten, J. A. Zasadzinski, *Langmuir*, 2006, **22**, 2465; (*c*) M. Suzuki, M. Yumoto, H. Shirai and K. Hanabusa, *Chem. Eur. J*., 2008, **14**, 2133; (*d*) H. Basit, A. Pal, S. Sen and S. Bhattacharya, *Chem. Eur. J*., 2008, **14**, 6534.
12. (*a*) G. O. Lloyd and J. W. Steed, *Soft Matter*, 2011, **7**, 75; (*b*) L. Meazza, J. A. Foster, K. Fucke, P. Metrangolo, G. Resnati and J. W. Steed, *Nature Chem*., 2013, **5**, 42; (*c*) X. Q. Dou, P. Li, S. Lu, X. Tian, Y. Tang and J. D. Mercer-Chalmers, *J. Mol. Liq*., 2013, **180**, 129.
13. N. Kakiuchi, T. Shoji, K. Hirasada, K. Matsumoto, H. Yamaguchi, US Patent, 0 253 012, October 4, 2012.
14. When the PalNa concentration increased up to X = 70 %, a hydrogel could not be obtained. Thus, the experimental data for X more than 50 % was not provided.
15. G. M. Kavanagh and S. B. Ross-Murphy, *Prog. Polym. Sci*., 1998, **23**, 533.
16. (*a*) W. K. Surewicz, H. H. Mantsch and D. Chapman, *Biochemistry*, 1993, **32**, 389; (*b*) N. Yamada, K. Ariga, M. Naito, K. Matsubara and E. Koyama, *J. Am. Chem. Soc*., 1998, **120**, 12192; (*c*) J. T. Pelton and L. R. McLean, *Anal. Biochem*., 2000, **277**, 167; (*d*) B. P. Rios, *Biochemistry*, 2001, **40**, 9074; (*e*) J. P. Schneider, D. J. Pochan, B. Ozbas, K. Raiagopal, L. Pakstis and J. Kretsinger, *J. Am. Chem. Soc*., 2002, **124**, 15030; (*f*) L.

E. Valenti, M. B. Paci, C. P. De Paili and C. E. Giacomeli, *Anal. Biochem*., 2011, **410**, 118.
17. As a result of the alkyl chain incorporation, the carboxylates in PalNa should become closer to the peptide residues in PalGH. Such would change the strength of the hydrogen bonding among the amide moieties and the protonation state of the carboxylate in PalGH, as observed by Fourier-transform infrared (FT-IR) spectroscopy.
18. (*a*) S. Hanski, S. Junnila, L. Almásy, J. Ruokolainen and O. Ikkala, *Macromolecules*, 2008, **41**, 866; (*b*) Y. Wang, W. Li and L. Wu, *Langmuir*, 2009, **25**, 13194; (*c*) B. Dong, T. Sakurai, Y. Bando, S. Seki, K. Takaishi, M. Uchiyama, A. Marunaka and H. Maeda, *J. Am. Chem. Soc*., 2013, **135**, 14797.
19. M. H. Bulter and M. F. Bulter, *Langmuir*, 2013, **19**, 10061.
20. O. Glatter, in Small-Angle X-ray Scattering, ed. O. Glatter and O. Kratky, Academic Press, London, 1982.
21. (*a*) P. Terech, N. M. Sangeetha, B. Demé and U. Maitra, *J. Phys. Chem. B*, 2005, **109**, 12270; (*b*) S. Roy, A. Dasgupta and P. K. Das, *Langmuir*, 2007, **23**, 11769; (*c*) G. Cheng, V. Castelletto, R. R. Jones, C. J. Connon and I. W. Hamley, *Soft Matter*, 2011, **7**, 1326; (*d*) P. Duan, L. Qin, X. Zhu and M. Liu, *Chem.–Eur. J*., 2011, **17**, 6389.
22. C. Tang, A. M. Smith, R. F. Collins, R. V. Ulijin and A. Saiani, *Langmuir*, 2009, **25**, 9447.
23. P. Greenspan, E. P. Mayer and S. D. Fowler, *J. Cell Biol*., 1985, **100**, 965.
24. (*a*) M. C. A. Stuart, J. C. van de Pas and J. B. F. N. Engberts, *J. Phys. Org. Chem*., 2005, **18**, 929; (*b*) C. B. Minkenberg, L. Florusse, R. Eelkema, G. J. M. Koper, and J. H. van Esch, *J. Am. Chem. Soc*., 2009, **131**, 11274; (*c*) J. H. Ryu, R. Roy, J. Ventura and S. Thayumanavan, *Langmuir*, 2010, **26**, 7086; (*d*) M. C. Morán, M. G. Miguel and B. Lindman, *Soft Matter*, 2011, **7**, 2001.
25. The smaller size of the fibrils may be due to the relatively weak interaction between the lamellar-like assmblies.
26. When sodium caprylate (CapNa) was used as an alternative to PalNa, the appearance of the hydrogel with X = 50 % was opaque, being similar to that of the homo PalGH hydrogel. CLSM observation revealed that the fibril network was unchanged upon the addition of CapNa. These results implies that the modulation of the molecular assembly is based on the incorporation of alkyl groups of PalNa into the PalGH assembly.
27. (*a*) F. C. MacKintosh, J. Käs and P. A. Janmey, *Phys. Rev. Lett*., 1995, **75**, 4425; (*b*) Y. S. Dagdas, A. Tombuloglu, A. B. Tekinay, A. Dana and M. O. Guler, *Soft Matter*, 2011, **7**, 3524.
28. (*a*) M. A. Greenfield, J. R. Hoffman, M. O. de la Cruz and S. I. Stupp, *Langmuir*, 2010, **26**, 3641; (*b*) P. Chakraborty, P. Bairi, B. Roy and A. K. Nandi, *ACS Appl. Matter. Interfaces*, 2014, **6**, 3615.